12-4-2018

Nanocapsules on a Lipid Membrane

Zain-Al-Abidin Shahid Kinnare

NANOCAPSULES ON A LIPID MEMBRANE

by

Zain-Al-Abidin Kinnare

A Thesis

Submitted in Partial Fulfillment of the

Requirements for the Degree of

Master of Science

Major: Physics

The University of Memphis

December 2018

Abstract

Nanoparticle technology is gaining traction in many different industries, particularly in imaging and the medical industries, and thus it becomes increasing important to understand how particles will affect the body. This is why we want to look at the way nanoparticles interact with lipid membranes, since lipids play vital roles in biological processes such as stabilizing the distal airways in our lungs in low volume situations. Knowing how nanoparticles will interact with these lipids can give us insights into the potential cytotoxicity of the particles, and how other agents, such as viruses act near/on a lipid membrane. In this thesis, we look at Nanocapsules, to determine the way they dock and aggregate on a lipid membrane.

Table of Contents

Chapter 1: Introduction

Lipid molecules are composed of three portions. One portion is polar and thus hydrophilic called the head group. The other two portions are hydrophobic hydrocarbons known as tail groups. Due to this construction, when placed in aqueous solution, the lipids quickly self-assemble into bilayers, where the tail groups are shielded from the water by the head groups. The bilayer and different proteins comprise the plasma membrane, which plays an important role in many biological processes. [28] [37]

At low temperatures, the bilayer is in gel phase, and transitions to a fluid phase as temperature rises. In the fluid phase, the membranes allow for transport of a large variety of transmembrane proteins, which act as gateways for other substances to pass through the membrane. In the fluid phase, membranes also can more easily deform allowing for process such as endocytosis, which is a form of active transport of molecules into a cell. [31] [62]

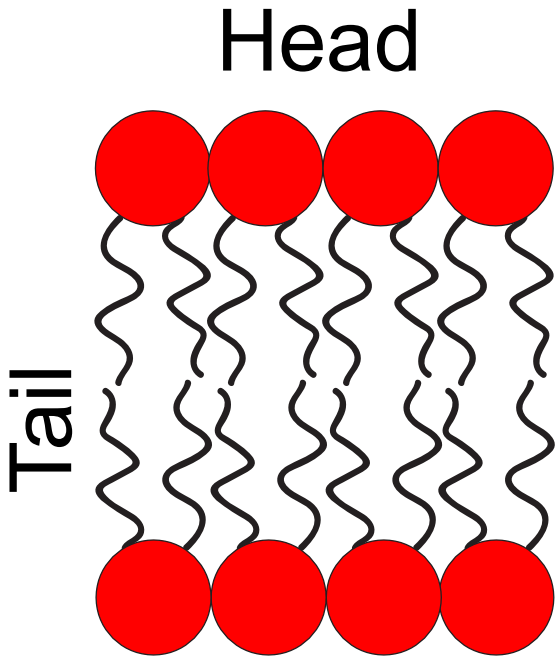

Figure 1: Representation of lipid bilayer, denoting head and tail groups

The two separate layers of the of the lipid bilayer membrane, are not symmetric with each other. [63] [64] The shape of the membrane, especially in vesicle form, is dramatically affected by the asymmetry, in conjunction with factors like temperature and the size of the vesicle.[65] While the molecule chain in each layer is held together by covalent bonds, the structure is held together by forces such van der Waals forces, which are much weaker, granting movement in the plane of the membrane. [30] [54] Membranes that form in places such as alveolus have tight membranes, however, other pulmonary surfactants can be much looser. Many pulmonary surfactants are composed of phospholipids, neutral lipids, and proteins, and the phospholipids are the ones that form the film at the interface between liquid and air. The goal of these of membranes is provide efficient gas follow, while optimizing the interaction with other molecules. [33] Knowing how these surfactants function, interact, and form have already been immensely useful in therapeutic trials for infants with Respiratory Distress Syndrome. [34]

The self-aggregation of lipids makes an appearance in many very important parts of animal biology. For example, pertaining to the lungs, a complex of lipids and proteins stabilize the distal airways in low volume situations. [32] And since lipids play a vital role in our bodies, and are found almost everywhere in our bodies, it becomes important to determine how different elements will affect them. In the case of the above example, researchers compare the aggregation of lipids when their aggregation is induced by SP-A proteins to aggregation induced by Ca^{2+}.[32][35][36] This type of aggregation will also very through the use of different proteins as well.[58]

Lipid Bilayers can take many different forms. An important form in the study of bilayers is the vesicle. A vesicle is a comprised of a fluid surrounded/enclosed by a lipid bilayer. These can form from processes like secretion and endocytosis. [55] This is a unique property of lipids

because it allows for the encapsulation many different solutes. [38] These vesicles also allow lipids to traverse different barriers in the body, in particular the skin. This makes lipid vesicles attractive for topical skin applications. [39][40] The vesicles can also pass through the plasma membrane through endocytosis, but also through fusing with the plasma membrane (this path is especially true for lipid vesicles primarily composed of phospholipids). [41][46] With these situations, we are primarily dealing with the lipid bilayers interacting with larger substances, but other end of the spectrum also provides valuable insight which is focused on more heavily in the later sections. A quick example is of anisotropically curved nanoparticles binding to lipid vesicle, and the subsequent aggregation of the nanoparticles that occur. This is also true for proteins. The membrane portion of these vesicles are comprised of amphiphilic molecules that aggregate and cause deformations to the membrane, that result in budding process. This can potentially rupture the membrane. [56][57] Computational research is being conducted to better understand this process. [43]

These same principles apply to lipids aggregating on materials that are not commonly found in the body. Self-assembly of synthetic lipids have been observed on carbon nanotubes, which seems to mimic the assembly properties of single-chain lipids that are used for immobilization of histidine-tagged proteins. [42] A similar coating process is used for drug treatment for cancer. [66]

It is important to note, these membranes and vesicles are comprised of different types of lipids from phospholipids to neutral lipids like cholesterol, as well as containing different proteins. Certain proteins, based on their adhesion strength to the membrane, can curve the membrane, and are also aggregated together on the membrane (something that is very difficult to characterize experimentally). [44] These are specialized proteins that aid in membrane remodeling

process, that is essential for tasks such as endocytosis and protein sorting. There have been coarse-grain models that aim at showing the attractive interaction (particularly aggregation) can occur purely due to the curvature of the membrane. [47] This curvature is not only affected by proteins. Lipid composition, nanoparticles, and viruses can play a larger role in the shape of lipid membrane. [45] [48] [49] [59] [60] [67]

Viruses take advantage of the way that proteins behave in on lipid membrane. Influenza's M2 protein is studied to understand it's functional mechanism in channeling protons to break down hydrogen bonds in histidine pairs. [50] [53] [61] Other viruses, such as West Nile, have lipid envelopes, which are comprised of the host cells membrane, around the virus's protein capsid. [51][52] The project here is to focus more on different nanoparticles. This is explained further in the following sections.

Nanomaterials

Over the last two decades, there has been an increase in research dealing with nanomaterials ranging from medicine to nanoelectronics. This has fostered research many different types of nanomaterials such as magnetic nanoparticles[13][17], polymer-based nanocapsules, quantum dots[14] and more.[15] Because of their size and other properties such as attraction to the head (antimicrobial) groups of a lipid, many of these materials can deform and/or penetrate a lipid membrane, and thus get entry into a cell. For example, Gold nanoparticle-based antibiotics can kill bacteria like E. coli, while also having the bacteria become more susceptible to the antibiotic. The belief is that the gold nanoparticle antibiotic is targeting the E. coli at the cell division pathway. This also implies that there might be higher barriers that will prevent resistance to evolve for the nanoparticle antibiotic versus its larger

counterpart. [1] This may be due to their size. Since nanoparticles are similar in size to materials like proteins and viruses [21], and since they can exhibit a high surface area to volume ratio, nanoparticles are able to bond to cell membrane, as well as pass through using the process of endocytosis. This warrants the study of the nanoparticles with both the cell and the membrane surrounding the cell. Gold nanoparticles, also, due to their plasmon-resonant absorption and scattering in the near infrared, are great probes and contrast agents for both in vivo and in vitro imaging. [10]

There are several factors that will affect the membranes deformation and penetration, such as the NP's density on the membrane and their solubility. Since NP's are able to have high surface area to volume ratio, the surface of the NP can be coated with different functional groups that would aid the process of tracking and binding to cells, ultimately allowing for targeted drug delivery and fluorescent biological labels.

As nanomaterials become more prevalent, their cytotoxicity becomes more and more of a concern, which is still poorly understood. Carbon nanoparticles, for example, have been getting a lot of attention due their light weight, tensile strength, as well as their thermal and chemical properties.[2][3] With these nanoparticles in particular, their shape, size, charge, surface chemistry, complexity, as well as a myriad of other factors play a role in the potential toxicity.[11] Another example is quantum dots. Even though they are composed of toxic elements, the use of quantum dots in the medical field seems to be bearing fruit. Certain types of quantum dots have been shown to affect the osmotic equilibrium of a cell. Also peptide-coated QD's have been shown to accumulate in the liver and spleen, in addition to the targeted area.[4] This shows that it is important to properly study the affects of these nanoparticles to minimize the dangers that they can have on human health. [11]

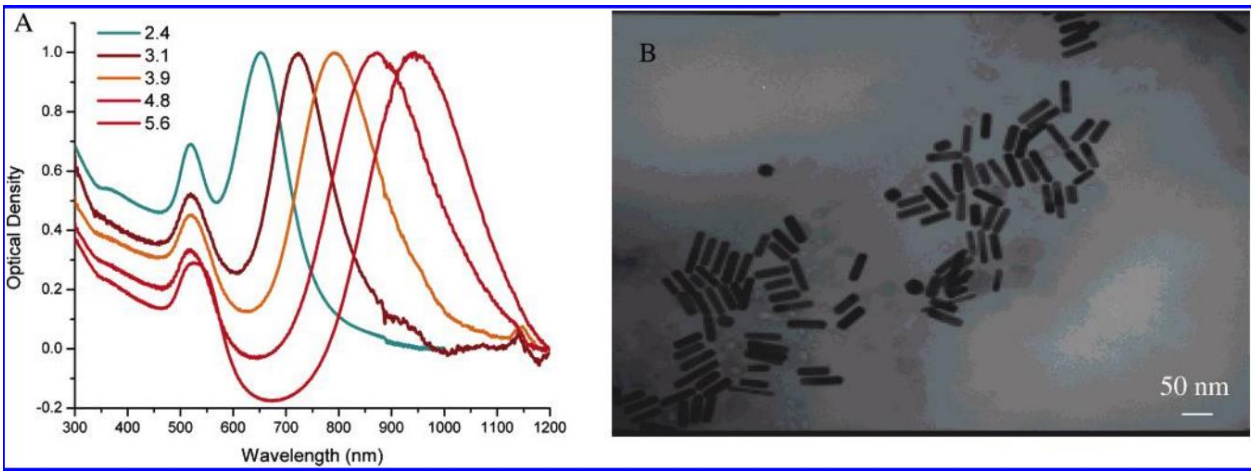

Figure 2: This is from Xiaohua Huang's paper "Cancer Cell Imaging and Photothermal Therapy in the Near-Infrared Region by Using Gold Nanorods" showcasing the optical strengths of gold nanorods. [5]

NanoSpheres

Several types of nanoparticles are studied interacting with these bilayers, nanospheres in particular have been looked at. These nanoparticles are absorbed into the cell through a process called endocytosis. For passive endocytosis, a ligand-coated nanoparticle can be used to model how a virus would interact on a cell membrane. When considering nanospheres interacting with a bilayer, factors ranging from size, attraction strength, to density of particles will determine the way the nanospheres will interact with membrane. [19] If there is only one sphere, these factors will determine the amount of wrapping the sphere will experience, whether it will endocytosis, and how much the membrane will deform. One of the determining factors of whether spontaneous endocytosis will happen, is if endocytosis will reduce the free energy of the system. In previous simulations, nanospheres that are comparable in size to the bilayer have shown that the adhesion of the nanoparticles to a bilayer causes the lipids in direct contact with nanoparticle to have a higher conformational order, further meaning that the bending rigidity increases when you add a nanoparticle to the membrane. In conjunction with this, these systems have partially wrapped states that are also thermodynamically equilibrium states. [6]

As we add particles, it will cause clustering and aggregation depending on number of particles. Depending on number of particles, the adhesion energy between the membrane head particles and nanoparticle, the density of the lipids, the aggregation of the nanospheres can take many different forms, from tubes chains to rings and v-shapes. For moderate values of the bending modulus nanoparticles will form into linear chains, while for low bending modulus, they will take up a triangular lattice. [6]

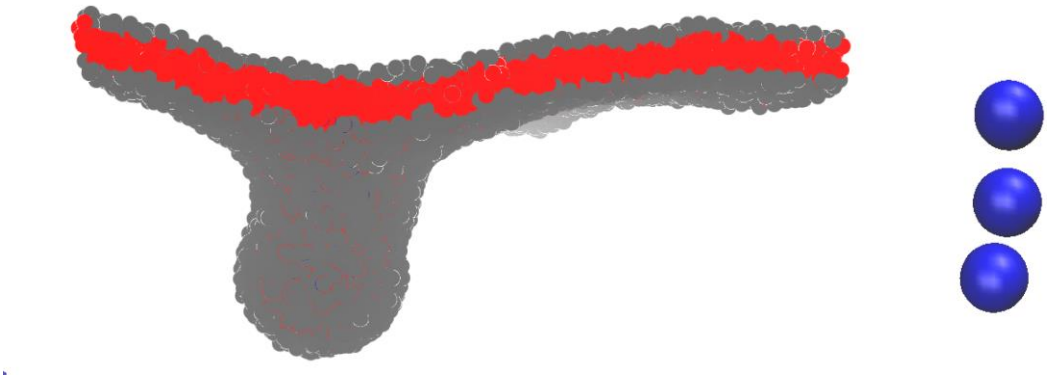

Figure 3: This is an example of the aggregation of nanosphere simulated by Eric Spangler, on a lipid membrane that is much larger than the size of the spheres. The image on the right turns off the visibility of the membrane

Non-Spherical Nanoparticles

In the sphere case, the size of the particle has been studied to see its effects on endocytosis. As we being to look at rods and capsules. The shape also begins to play an important role in determining the endocytic pathways that the nanoparticle will take. It is important to understand these effects because it helps determines the positive and negative factors about cytotoxicity the nanoparticle. For example, gold nanorods are being studied as method of targeted cancer therapy. The internalization pathways for these gold nanorods has an impact on their bioactivity. The way that the gold nanorods are absorbed by cancer cells, stem cells, and normal cells is important to determine what causes the difference in cytotoxicity between these three cells. In this case, the pathways were similar, which suggested intracellular localization was the deciding factor in the fate of the cancer cells rather then the endocytic pathway. [7] These gold nanorods uptake into the cell has been shown to decrease as the aspect ratio of the nanorod increases. [12]

For nanocapsules, there have been studies done using a ligand-receptor model, where the membrane is 2D, to study the endocytic pathways a nanocapsule will follow. Having a 2D membrane is way to understand how a nanoparticle that is very larger compared to the membrane and is much bigger than the width of the membrane will interact with said membrane. In these studies, it determined that the size of the nanoparticle determines whether or not endocytosis will complete, while the shape will determine the path. The shape, in this case, refers to the aspect ratio of the length to the radius of the nanocapsule. As the shape is made more and more elongated, the particle initially lays down on the membrane, and as it gets wrapped, it is rotated to the vertical position, until finally separating from the membrane. [8]

This concept of the shape of a nanoparticle effecting the wrapping involved, is also true for ellipsoid particles (Both oblate and prolate). Looking at only the wrapping of the

nanoparticle, and not the endocytosis, as particles shape changes from a oblate ellipsoid to a prolate ellipsoid, the bending energy for a wrapping membrane decreases, but as the prolate ellipsoid begins to the thin out, there is gradual climb in the bending energy. [9]

Objectives

The way that spherical nanoparticles are wrapped and how they aggregate on a membrane has been studied heavily. Nanorods have also been investigated in a similar regard. There is an understanding in the formations that occur when these nanoparticles are placed on lipid bilayer. The goal of this research project was to look at the nanocapsules, a cylinder with hemisphere caps on both ends. We wanted to investigate how several factors determined the wrapping of the nanocapsules, such as the length, radius, and number of particles. These particles resemble the use of certain bioconjugates on bacteria such as E. coli and provide a way to study aggregation within that context. And while there have been studies that have looked at the endocytic pathway of similarly shaped particles, albeit much at much larger length scales, this study aims to look at the wrapping and aggregation of the nanocapsules

Chapter 2: Model and Numerical Method

Lipid Molecules are comprised of one head group and two tail groups. The head groups are hydrophilic, and the tail groups are hydrophobic. In this model, each of these groups are represented by a soft ball. Similarly, the nanoparticles are constructed from small balls similar to that of the lipid head and tail particles. There are harmonic interactions that deal with the bond between the lipid balls as well as the balls of the nanoparticle. A three-body interaction is calculated to determine the bending rigidity of the lipid, and two body interaction is used to determine the potential between neighboring balls. These three interactions contribute to the interaction potential, which is given by the following equation. (6)

$$\mathrm{U}(\{\mathbf{r_i}\}) = \sum_{i,j} U_0^{\alpha_i\alpha_j}(r_{ij}) + \sum_{i,j} U_{bond}^{\alpha_i}(r_{i,i+1}) + \sum_{i,j} U_{bend}^{\alpha_i}(r_{i-1}, r_i, r_{i+1}) \tag{1}$$

$\sum_{i,j} U_0^{\alpha_i\alpha_j}(r_{ij})$ is a two body interaction between two particles, i and j, and is given by

$$\sum_{i,j} U_0^{\alpha_i\alpha_j}(r_{ij}) = \begin{cases} \dfrac{(U_{max}^{\alpha\beta} - U_{min}^{\alpha\beta})(r_m - r)^2}{r^2} + U_{min}^{\alpha\beta} & if\ r \le r_m \\ -2U_{min}^{\alpha\beta}\dfrac{(r_c - r)^3}{(r_c - r_m)^3} + 3U_{min}^{\alpha\beta}\dfrac{(r_c - r)^2}{(r_c - r_m)^2} & if\ r_m < r \le r_c \\ 0 & if\ r > r_c \end{cases} \tag{2}$$

,where $U_{max}^{\alpha\beta} > 0$ for a given pair (α, β), r_m is the equilibrium distance, and r_c is the cut-off distance. When $U_{min}^{\alpha\beta}$ is negative, there is a short-range attraction between two of type α and β, where α and β can be a tail, head, or nanoparticle ball. This is only the case when both are tail balls, or one is a head ball and the other is a nanoparticle ball, otherwise $U_{min}^{\alpha\beta} = 0$. This allows for the stable formation of lipid bilayers, and for the adhesion of the nanoparticles to the bilayer. (6)

$U_{bond}^{\alpha\beta}(r)$ is the harmonic interaction for bonds between balls of the lipid molecule and the bonds between the balls of the nanoparticle. This is given by,

$$U_{bond}^{\alpha\beta}(r) = \frac{k_{bond}^{\alpha\beta}}{2}\left(r - a_b^{\alpha\beta}\right)^2 \tag{3}$$

, "where $k_{bond}^{\alpha\beta}$ is the bond stiffness and $a_b^{\alpha\beta}$ is the preferred bond length" [6].

$U_{bend}^{\alpha_i}(r_{i-1}, r_i, r_{i+1})$ is the potential energy for the three-body interaction that determines the rigidity of the lipids, and is given by the following:

$$U_{bend}^{\alpha_i}(r_{i-1}, r_i, r_{i+1}) = \frac{k_{bend}^{\alpha_i}}{2}(cos\theta_o - \left(\frac{r_{i,i-1}\dot{r}_{i,i+1}}{r_{i,i-1}r_{i,i+1}}\right))^2 \tag{4}$$

, where $k_{bend}^{\alpha_i}$ is the bending rigidity constant and θ_o is the desired splay angle. [6]

The nanoparticles are arranged in a face-center-cubic lattice with stiff harmonic bonds. The lattice vectors for this structure are given by:

$$a_1 = \frac{a}{2}(0,1,1) \tag{5}$$

$$a_2 = \frac{a}{2}(1,0,1) \tag{6}$$

$$a_3 = \frac{a}{2}(1,1,0) \tag{7}$$

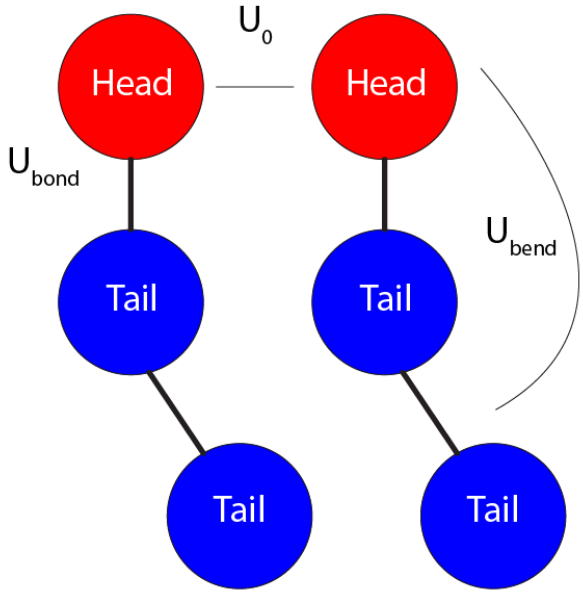

Figure 4: harmonic interactions for bonds inside the lipid, three body interaction for bending rigidity, and two body interaction between neighboring balls

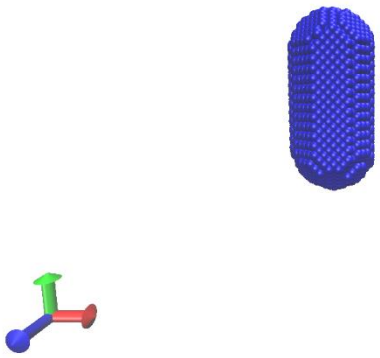

Figure 5: This is an example of a Nanocapsule of Radius = 3 and Length = 7

Figure 6: This is an example of the construction of the lipid bilayer. The red particles represent the tail particles, while the gray represent head particles.

Numerical Approach

In this model, Molecular Dynamics is used to move particles according Newtons Law of Motion in conjunction with a Langevin Thermostat. The Langevin dynamics mimics the presence of solvent. The equations of motion are given by,

$$\dot{r}_i(t) = v_i(t) \tag{8}$$

$$m\dot{v}_i(t) = -\nabla_i U(\{r_i\}) - \Gamma v_i(t) + \sigma\Theta_i(t) \tag{9}$$

, where is *m* is the mass of each ball, Γ is the coefficient of friction, and $\sigma\Theta_i(t)$ is a random force that keeps the system in thermal motion (representing a thermal bath), and is dictated by following correlation,

$$\langle\Theta_i(t)\rangle = 0 \tag{10}$$

$$\langle\Theta_i^{\mu}(t)\Theta_j^{v}(t')\rangle = \delta_{\mu v}\delta_{ij}\delta(t-t') \tag{11}$$

, where u, v represents *x*, y, or z components/direction. The random force keeps the system in thermal motion, and in conjunction with the dissipative force, it functions as the thermostat and achieves thermal equilibrium. In other words, Γ and σ are related using the fluctuation-dissipation theorem, giving $\Gamma = \frac{\sigma^2}{2k_bT}$. This insures that the fluctuations and dissipations negate each other over time. During each timestep of the simulation the Verlet-Velocity method is used to determine the equations of motion for each particle. (6)

Simulation Parameters

This model incorporates times, length, and energy as the base units. Verlet-Velocity is method that calculates both position and velocity in each step. Since, we want to keep our calculation in base units and focus on the scale of each parameter, we employ the Verlet-Velocity method with $\Gamma = \frac{\sqrt{6}m}{\tau}$, rather than the explicit form we have earlier, where *m* continues to be the mass of each ball, τ is the time scale and is given by $\tau = r_m \left(\frac{m}{\epsilon}\right)^{\frac{1}{2}}$, where r_m is the length scale, and ϵ is the energy scale.(6)

The lipid bilayers are composed of 20,000-60,000 lipid molecules. The bilayer is kept at constant zero tension, with a density of lipids, $\sigma \approx 3.11 r_m^{-2}$. The area of the membrane and the pressure are kept constant. (6)

Simulations are done at different adhesion strengths between the nanoparticles and the lipid heads, ranging from $|U_{min}^{nh}| = .1\epsilon \; to \; 1\epsilon$**.** Some of the simulations are done using an annealing process, where the U_{min}^{nh} is slowly raised to determine the transition point between to states of the system.. Below are the interaction values between particles in our simulations:(6)

$$U_{max}^{hh} = U_{max}^{th} = U_{max}^{nt} = 100\epsilon, \tag{12}$$

$$U_{min}^{hh} = U_{min}^{th} = U_{min}^{nt} = 0, \tag{13}$$

$$U_{min}^{tt} = -6\epsilon, \tag{14}$$

$$U_{min}^{nh} = -\mathrm{E}, \tag{15}$$

$$U_{max}^{tt} = U_{max}^{nh} = 200\epsilon, \tag{16}$$

$$k_{bond}^{ht} = k_{bond}^{tt} = \frac{100\epsilon}{r_m^2}, \tag{17}$$

$$k_{bond}^{nn} = \frac{2800\epsilon}{r_m^2}, \tag{18}$$

$$k_{bend}^{h} = 100\epsilon, \tag{19}$$

$$k_{bend}^{n} = 0 \tag{20}$$

$$r_c = 2r_m, \tag{21}$$

$$a_b^{ht} = a_b^{tt} = 0.7r_m, \tag{22}$$

$$a_b^{nn} = .35\, r_m. \tag{23}$$

Chapter 3: Results

Single Nanocapsule

The first case we considered is that of a single nanocapsule placed on a square lipid membrane constructed of 25,000 lipids to 50,000 lipids depending on the size of the nanocapsule. The membranes length is roughly 3 to 4 times the total length of the nanocapsule. This is done to ensure that there are minimal edge effects, since we use periodic boundary conditions.

In the initial set up for the membrane, the individual molecules are placed uniformly in the system. Once the system gets going, the membrane expands due to the interactions between all the molecules as well as do to the temperature of the system. If there was no nanoparticle on the membrane, it takes roughly 5,000 – 10,000 tau for the membrane to reach equilibrium (depending on the size of the membrane).

We determine whether the membrane has reached equilibrium by looking at the area of the membrane. The membrane is forced to stay in roughly a square shape, and as the simulation progresses, the membrane initially grows (preserving the square shape) and then begins to equilibrize in area, which coincides with the system reaching equilibrium. As stated previously, this take roughly 5,000 to 10,000 tau. Once we add in a nanoparticle, the same principle applies. The area of the membrane grows initially, but as the nanoparticle bounds with the membrane, and depending on how it is wrapped, or if there is a orientation change of nanoparticle, the membranes area can either shrink or grow. However, once the area equilibrizes, that is generally the final state of the system. With a single nanoparticle, this can happen in 20,000 to 40,000 tau depending on the size of the membrane and the size of the nanoparticle. There are other indicators for the equilibrium of a system such as the potential energy of the system reaching equilibrium.

Our initial look is at nanocapsules with a Radius = 3, and lengths ranging form a value of 1 to 20. Note that length refers to the length of the capsule between the two hemispheres and doesn't not include the length of the hemispheres. For example, a nanocapsule of radius = 3 and length = 1, would have a total length from end to end of 7. We place these nanoparticles, above the lipid membrane right below where the interaction cut off is. When the simulation begins, the nanoparticle drops to bind with the lipid membrane, and the depending on the $|U_{min}|$, will go under various amounts of wrappings and rotations.

In this initial look, we find that there is a phase transition for the single particle case. The first state is where the nanocapsule lays horizontally on the membrane, this is for lower values of $|U_{min}|$ and for higher values the nanocapsule gets in encapsulated by the membrane and in a vertical position, perpendicular to the plane of the membrane, as shown in Figure 7. We used an annealing process to determine where the transition between the two states happens. In this annealing process, we ran the simulation at particular $|U_{min}|$, generally a value that was confirmed to be in the horizontal state, and let the system reach equilibrium. We would then increase the $|U_{min}|$ by a step of .05, observe the change on the particle, let the system reach equilibrium, and repeat.

For lower values of $|U_{min}|$, roughly around .3 for most of the nanocapsules with radius of 3, the membrane experience very little deformation caused horizontally lying capsule. As the $|U_{min}|$ increases, this deformation also increases. The nanocapsule is wrapped more and more by the lipid membrane, and would stay relatively parallel to the plane of the membrane. When the $|U_{min}|$ get high enough, there is a sharp transition from the parallel state to the perpendicular state as shown in Figure 8. One end of the nanocapsule pushes down on the membrane, to go into the vertical state. As this happens the membrane on the side of the nanocapsule fills in around the

unwrapped portion on the nanocapsule, starting the at the descending end, almost in the zipper fashion. This process will only last at most 1,000 tau.

As can be seen, when the $|U_{min}|$ is before the transition point, the angle of the nanocapsule is close to 90 degrees with the z-axis, once the $|U_{min}|$ is raised to a sufficient value during the annealing process, the angle makes a sharp transition to being close to 0. Each $|U_{min}|$, is given 25,000 – 40,000 tau to ensure that equilibrium is reached for that value of $|U_{min}|$ during the annealing process. Figure 9, shows the $|U_{min}|$ for which this transition happens as a function of the length of the nanocapsule.

The way the angle is determined in for both Figure 8 and Figure 9 is by creating a vector that represents the Nanocapsule. The vector is determined from one end of the nanocapsule to the other end. This is done at every recorded time step after the completion of the simulation. This is then compared to the z-axis, using the dot product between the z-axis the nanocapsule vector. When the angle between the z-axis and nanocapsule is 90 degrees, the nanocapsule is in the horizontal state, and when the angle is 0 degrees, the nanocapsule is in the vertical state. This can be confirmed visually for majority of the nanocapsules. Nanocapsules with a length of 1 are harded to confirm visually.

When increasing the $|U_{min}|$ past the transition point, there is a neck that forms above the nanocapsule in the membrane. As the $|U_{min}|$ continues to rise, the neck pinches inward. This pinching continues until it closes off, and the nanocapsule finishes undergoing endocytosis. This process can shift up and down the curve depending on the radius of the caps on the nanocapsule as shown by Figure 19. As you increase the radius, the closer you get to endocytosis. The nanocapsule that is at a radius of 9 at a $|U_{min}| = .4$, has already experienced endocytosis, while

one of radius of 5 has only just entered the vertical state, and one that is of radius 3 would only still be in the horizontal state.

Multiple Nanocapsules

As we add more nanocapsules to the system, we studied the way that the nanocapsules aggregated on the membrane. Since we are using periodic boundary conditions, adding nanoparticles in principle means increasing the nanocapsule density on the the lipid membrane. With our intial look, we want to avoid high particle densities, and have our nanoparticles near the center of a lipid membrane much larger than the total length of the nanocapsules. In the case of two nanocapsules, they are placed on a membrane that ranges from 35,000 lipids to 70,000 lipids, and allowed to aggregate. The two nanocapsules meet at their ends, and at low values of $|U_{min}|$, they slightly deform the membrane around them with the largest deformation being at their aggregation point. As the $|U_{min}|$ increases the deformation increases as well, and the aggregation point of the two nanocapsules sinks into the membrane while the other ends of the capsules stay near the upper portion of the membrane. This forms a v-shape as shown in Figure 10. As the $|U_{min}|$ increases further the angle between the two nanocapsules decreases until they sink deep enough into membrane and the membrane forces them part. Portions of the membrane fill in-between the nanocapsules, starting above the aggregation point. During the process of the membrane separating the two nanocapsules, the angle between them increases, until they are separated and eventually made parallel. Figure 11 demonstrates this for two different length of nanocapsules. Figure 12, show the angle between the two nanocapsules vs $|U_{min}|$. Both figures show that there are two transition points in the two particle system. The first one occurs when the nanocapsules have been encapsulated enough to have the lipid membrane slip in-between them.

The second transition occurs when the membrane has split the nanocapsules apart, are separately encapsulated. But even in this case, the deformation that occurs above the nanocapsules on the membrane is still conjoined between the two nanocapsules. Even though they are both individually wrapped, the distance between the two nanocapsule is kept very small compared to the length of the nanocapsules.

In the beginning of the annealing process, where the two nanocapsules join and begin to dip into the lipid membrane, the shape the nanocapsules form is a v-shape. Due to the shape, and the connection point of the two nanocapsules, the possible shapes are limited to v-shapes with different angles. This also occurs in the spherical case, even though there are more degrees of freedom in the spherical case. Figure 13, shows a side by side comparison of the spherical case with the nanocapsules case. One way to understand this, is to view the nanocapsules as a series nanospheres. In this way, it makes sense, why there would be similar states between the two cases. This would also explain further similarities showcased later.

As we, add more nanocapsules to the system, they imbed themselves further into a v-shape, creating a smoother curve for the aggregation, becoming more of a u-shape and getting closer to having the same states as the sphere case. Figure 13, shows the comparison between the v-shape created by the 2 nanocapsules case and the v-shape created during nanosphere simulations, Figure 14, shows the comparison between a ring state for the nanospheres and the 3 nanocapsule case. This continues for more particles as well, the v-shape and u-shape continue to appear for the 4 nanocapsule case, 5 nanocapsule case, and 9 nanocapsule case as well. As we add more nanocapsules, the shape becomes smoother, although there are some situations that still have the sharp v-shape, generally when the number of nanocapsules is even. Looking at Figure 17, we see that there is a change between a v-shape to a u-shape as the $|U_{min}|$ increases

from .4 to .5. Similar to the two particle case, the nanoparticles are squeezed together forcing a rigid v-shape, but once they have been pushed in sufficiently and made a large enough deformation onto the lipid membrane, the membrane begins to fill in between the two arms of the v-shape to get a more complete encapsulation. Then like the two particle case, the filling in spreads the nanocapsules apart creating more of a ring/u-shape that also occurs in the spherical cases. This is further shown in Figure 18 and 19. As the $|U_{min}|$ increases, a more defined and narrow neck forms, the particles are more deeply invaginated, and the membrane pinches at center of the u-shape.

Another important aspect to note, in all of the case nanocapsules cases, once the particles have aggregated, they all form a neck that tends to persist as the $|U_{min}|$ increases, and tends to increase and becomes more prominent as the $|U_{min}|$ increases. It also narrows as $|U_{min}|$ increases. This is potentially the path that theses cases will take for endocytosis, once the neck narrows enough. We have seen this in the one particle case already. The way pathway for the endocytosis for the one particle case is that first it lays flat on the membrane, then transitions into a vertical state, where a neck forms and begins to thin until finally having the nanocapsule endocytose

When we add many more particles, such that the density of nanocapsules on the membrane is very high, we have these u-shapes and v-shapes link up to create long chains as shown in Figure 15. Note that all other simulations have been done such that the density of nanocapsules on the membrane are low. There is plenty of room on the lipid membrane for the other simulation for the edge effects of the periodic boundary conditions to be minimal. For the 29 particle case in Figure 15, this is not the case. The simulation in this case connects nanocapsules on opposite sides of the system, and the nanocapsules are spread through most the membrane. Much like the previous cases, the deformation caused by the nanocapsules increases

with $|U_{min}|$. Since there are many particles, the deformations is much larger for lower $|U_{min}|$ compared to other cases. This is better exemplified between the two, three, four, five, and nine particle cases. When there are more particles, the system in more deeply entrenched state compared to the fewer particle state. For example, for the value of $|U_{min}| = .5$, where membrane has already filled in between 4 nanoparticles of radius = 3 and length = 3, the two particle at the same conditions is still in the process of being squeezed together. Similar to how we can view a nanocapsule as a series of nanospheres, we can consider that the size of the particles has a cumulative effect. Each individual nanoparticle deforms the membrane a certain amount. Looking at the being of our simulation, nanoparticles are place randomly above the lipid membrane. Once they bind to the membrane, they cause their individual deformations to the membrane, and as the nanoparticles aggregate, the deformations merge.

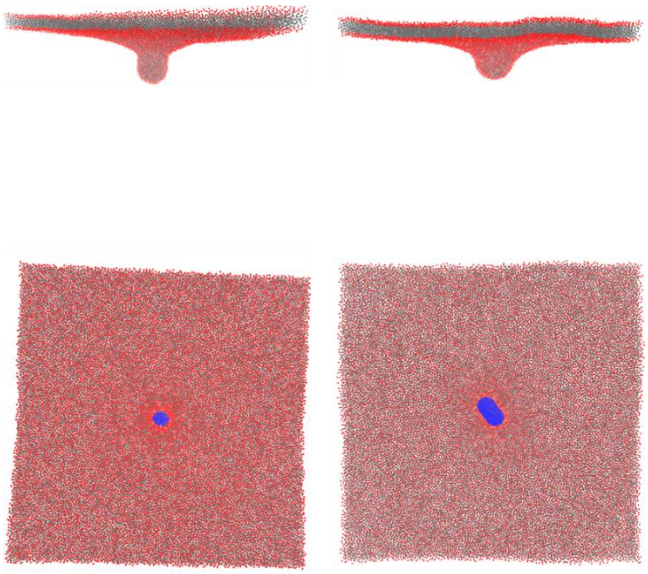

Figure 7: Above is a nanocapsule with Radius = 3 and Length = 3. The right two images are at $|U_{min}|$ = .5 (horizonatal state) and the left two images are at $|U_{min}|$ = .7 (Vertical State)

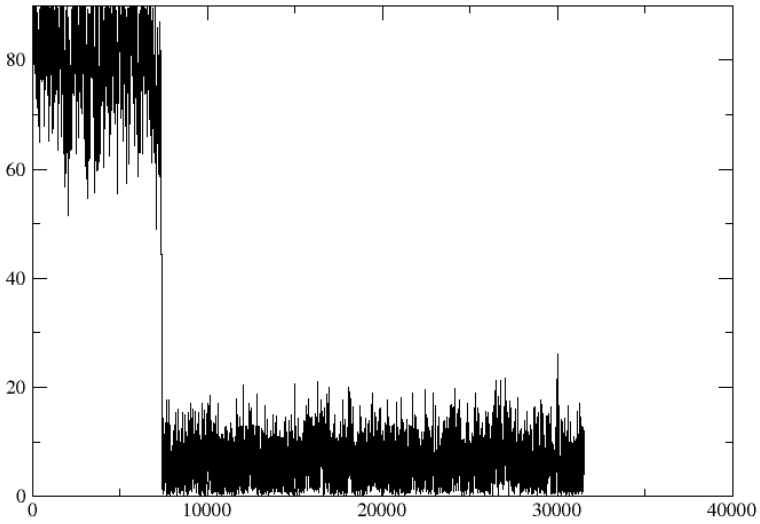

Figure 8: This is graph of Angle vs Time(10 Tau). This is for a nanocapsule of Radius = 3 and Length = 3. Each value of $|U_{min}|$ goes through 25,000 tau. This graph shows a sharp transition at $|U_{min}|$ = .65 at Time(approx.) = 76,000 tau

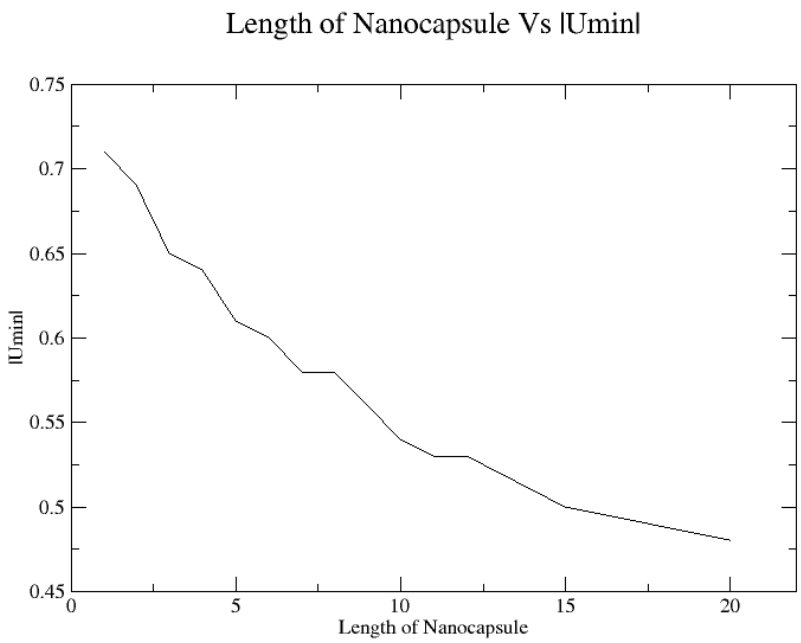

Figure 9: This is a graph of Length vs $|U_{min}|$, for when a nanocapusle will undergo the transition from horizontal to vertical. All of the nanocapules used for this graph had a Radius = 3. Any $|U_{min}|$ - length combination along and above the curve will be in the vertical state, while below the curve will produce the horizontal case

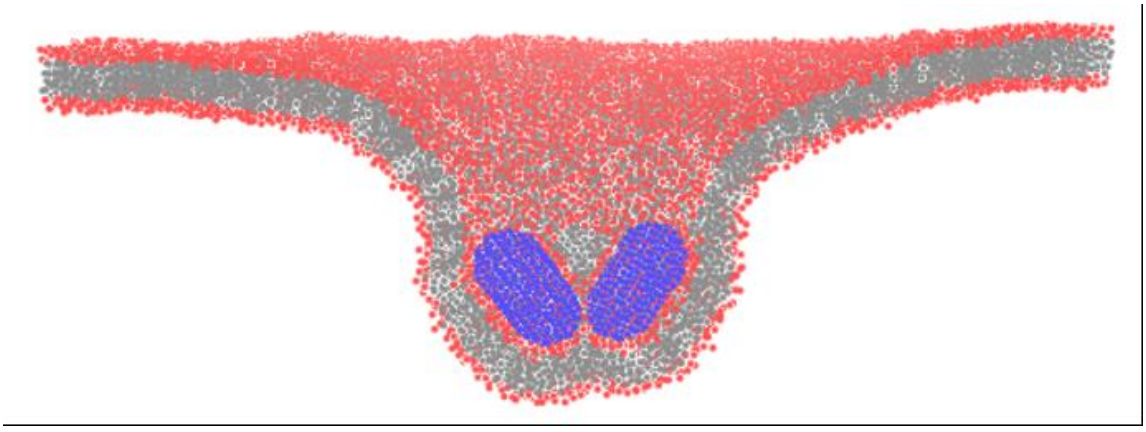

Figure 10: Two Nanocapsule of Radius = 3 and Length = 3 at $|U_{min}|$ = .6 aggregated in v-shape configuration

Figure 11: The right set of images are of two nanocapsules of Radius =3 Length = 9. The left images are of Radius = 3 and Length = 7. Both sets range from $|U_{min}| = .5$ to $|U_{min}| = .9$, with increasing $|U_{min}|$ as you proceed down the images.

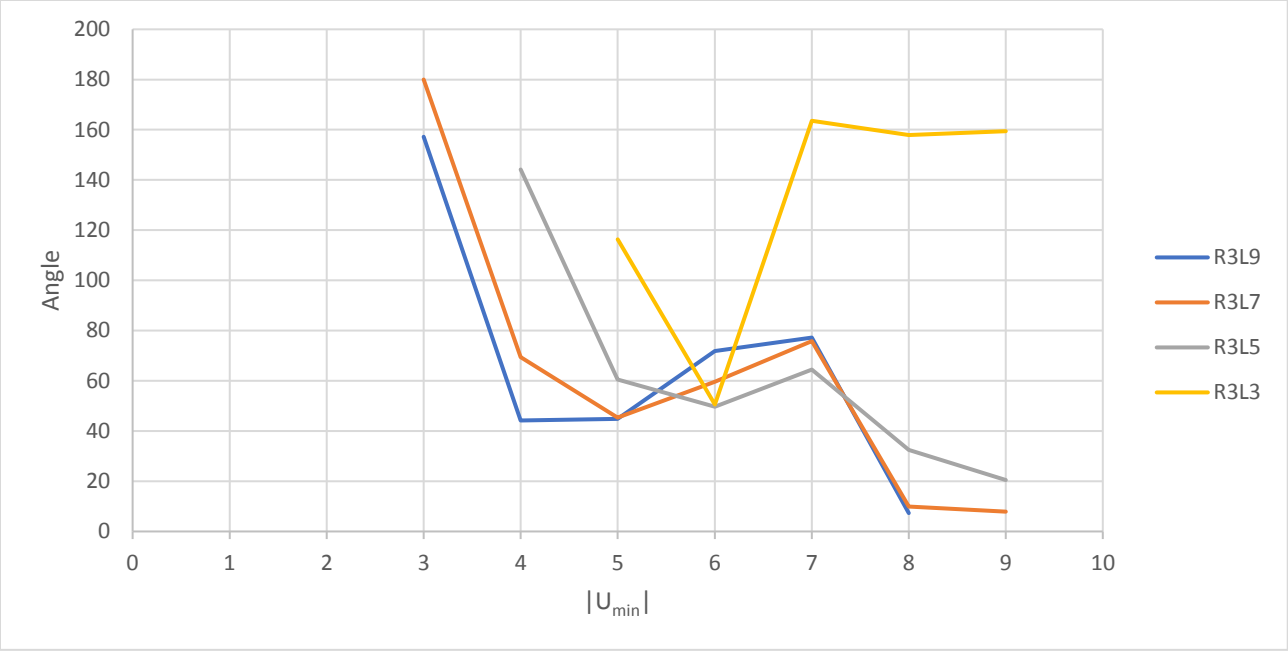

Figure 12: This shows the angle between two nanocapsules as a function of $|U_{min}|$. All of Nanocapsules are of Radius 3, and the lengths are 3,5,7, and 9 as indicated by the legend.

Figure 13: This is a comparison between sphere simulations done by Eric Spangler and the two nanocapsule case (Radius = 3, Length = 3, $|U_{min}| = .5$).

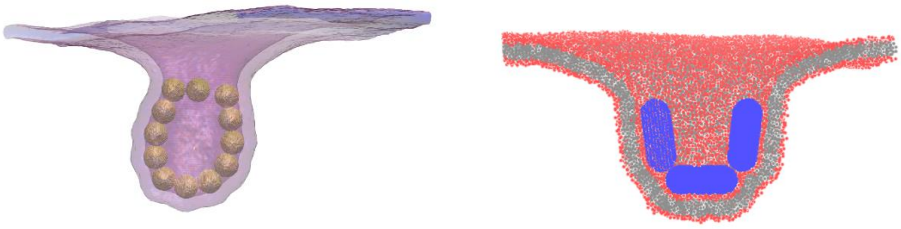

Figure 14: This is a comparison between sphere simulations done by Eric Spangler and the three nanocapsule case (Radius = 3, Length = 5, $|U_{min}| = .5$).

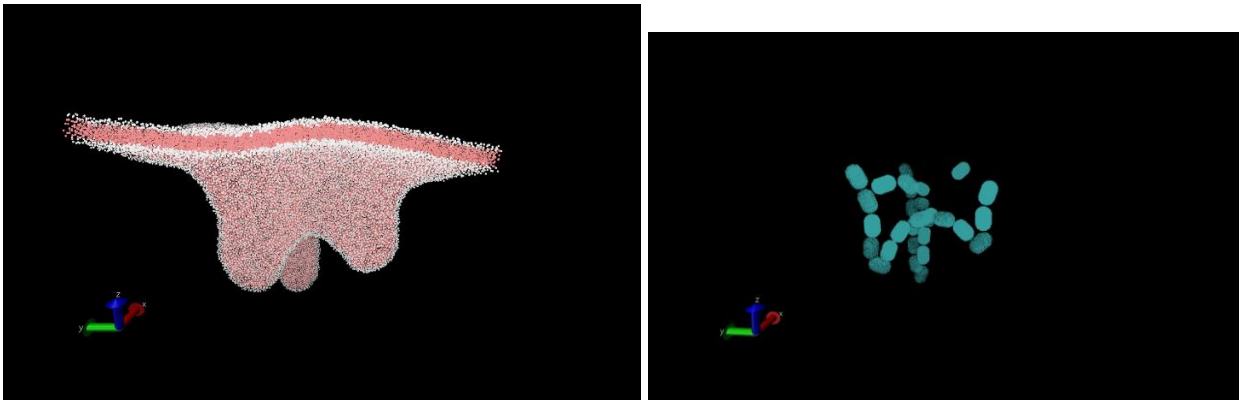

Figure 15: This is an example of 29 Nanocapsules of Radius = 3 and Length = 3 where the density of nanocapsules on the membrane is high

Figure 16: This is an example of a 9 Nanocapsules of Radius = 3 and Length = 3. The left image is at $|U_{min}| = .6$ and the right image $|U_{min}| = .7$

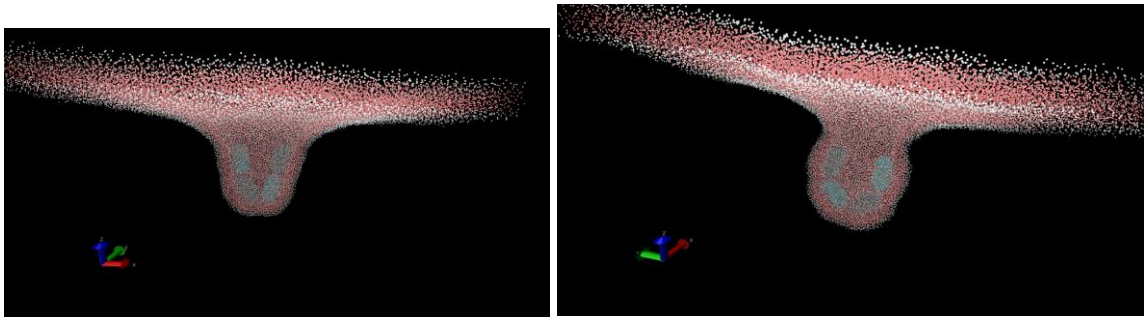

Figure 17: This is an example of a 4 Nanocapsules of Radius = 3 and Length = 3. The left image is at $|U_{min}| = .4$ and the right image $|U_{min}| = .5$

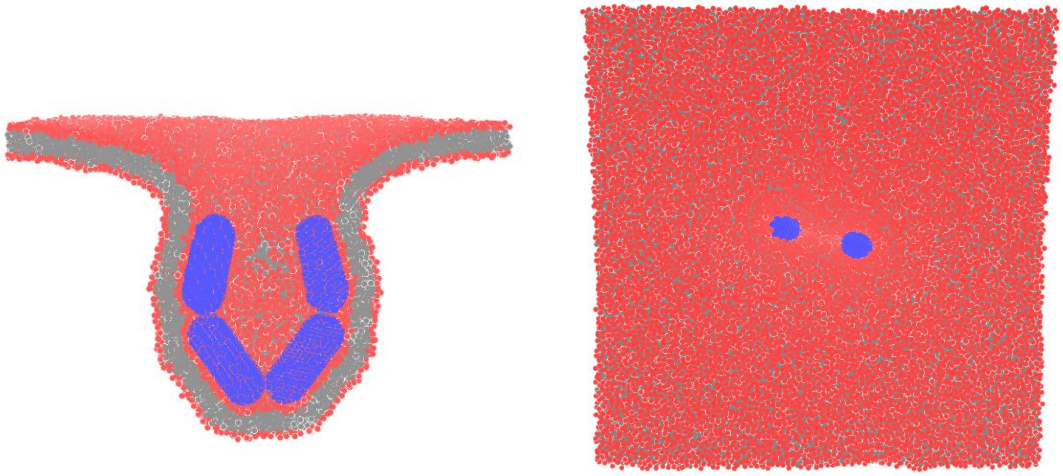

Figure 18: This is an example of a 4 Nanocapsules of Radius = 3 and Length = 9 at $|U_{min}| = .5$

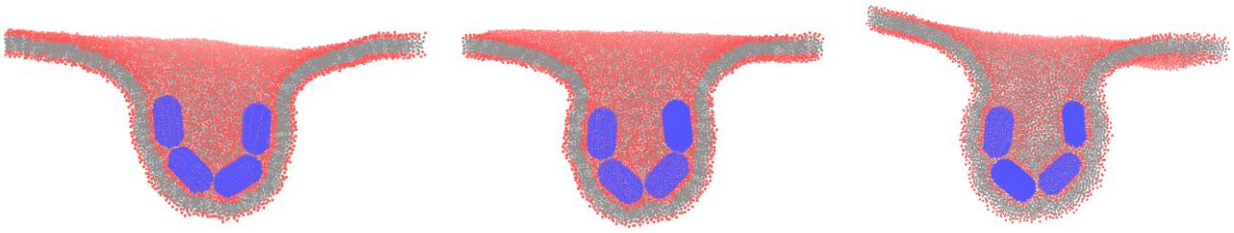

Figure 19: This is an example of a 4 Nanocapsules of Radius = 3 and Length = 5. From Left to Right the $|U_{min}| = .5$, $|U_{min}| = .6$, $|U_{min}| = .7$

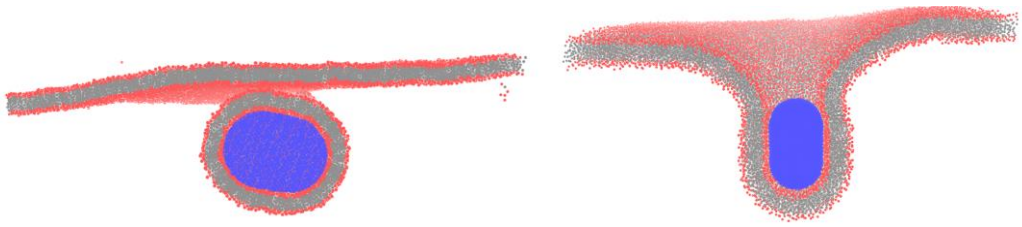

Figure 20: The left image is Radius = 9 and Length = 7, and right image is at the same length at Radius = 5. Both are at $|U_{min}| = .4$

Chapter 4: Conclusion

Nanomaterials provide a wide range of unique properties that can aid in treatment of virus and strengthen current imaging techniques. They can potentially play a very important role in new medical techniques. For this reason, knowing how they will interact in the body becomes very important.

When determining how they will interact in the body, notions of shape and adhesion potential energy become very important. Some important shapes are spheres, rods, and capsules. This project took a look at capsules to determine the way they will interact with a lipid membrane that is much larger than the nanoparticle. In the one particle case, we determined that there was a phase transition as you increase the adhesion strength between the nanocapsules and the lipid head groups. The transition was for the nanocapsule lying flat on the membrane to being vertically engulfed by the membrane. This resembled the tube shape that can occur when multiple nanospheres are wrapped by a lipid membrane as shown in Figure 3. As we added more particles, the resemblance to the sphere can increases. Two nanocapsules produce a similar v-shape that can occur in the nanosphere case as well. This continues as we add more nanoparticles. The shape more closely resembles other configurations you would see in the sphere case. The number of nanocapsules will also determine how smooth that shape will be. This shows us that there is similarity on how the nanocapsules and the nanospheres are treated on the lipid bilayer and implies that the nanocapsule can be thought of as many nanospheres connected. Although, that notion does not fully complete the picture of how the nanocapsules will behave, since they have additional rigidity, it does provide a closer look at the elements in play during the interaction between nanocapsules and lipid membranes.

References

(1) Eum, N. S., Yeom, S. H., Kwon, D. H., Kim, H. R., & Kang, S. W. (2010). Enhancement of sensitivity using gold nanorods—Antibody conjugator for detection of E. coli O157: H7. *Sensors and Actuators B: Chemical*, *143*(2), 784-788.

(2) Liu, H., Ye, T., & Mao, C. (2007). Fluorescent carbon nanoparticles derived from candle soot. *Angewandte Chemie International Edition*, *46*(34), 6473-6475.

(3) Schuster, J., He, G., Mandlmeier, B., Yim, T., Lee, K. T., Bein, T., & Nazar, L. F. (2012). Spherical ordered mesoporous carbon nanoparticles with high porosity for lithium–sulfur batteries. *Angewandte Chemie*, *124*(15), 3651-3655.

(4) Dubertret, B., Skourides, P., Norris, D. J., Noireaux, V., Brivanlou, A. H., & Libchaber, A. (2002). In vivo imaging of quantum dots encapsulated in phospholipid micelles. *Science*, *298*(5599), 1759-1762.

(5) Huang, X., El-Sayed, I. H., Qian, W., & El-Sayed, M. A. (2006). Cancer cell imaging and photothermal therapy in the near-infrared region by using gold nanorods. *Journal of the American Chemical Society*, *128*(6), 2115-2120.

(6) Spangler, E. J., Upreti, S., & Laradji, M. (2016). Partial wrapping and spontaneous endocytosis of spherical nanoparticles by tensionless lipid membranes. *The Journal of chemical physics*, *144*(4), 044901.

(7) Wang, L., Liu, Y., Li, W., Jiang, X., Ji, Y., Wu, X., ... & Li, Y. (2010). Selective targeting of gold nanorods at the mitochondria of cancer cells: implications for cancer therapy. *Nano letters*, *11*(2), 772-780.

(8) Huang, C., Zhang, Y., Yuan, H., Gao, H., & Zhang, S. (2013). Role of nanoparticle geometry in endocytosis: laying down to stand up. *Nano letters*, *13*(9), 4546-4550.

(9) Bahrami, A. H., Raatz, M., Agudo-Canalejo, J., Michel, R., Curtis, E. M., Hall, C. K., ... & Weikl, T. R. (2014). Wrapping of nanoparticles by membranes. *Advances in colloid and interface science*, *208*, 214-224.

(10) Tong, L., Wei, Q., Wei, A., & Cheng, J. X. (2009). Gold nanorods as contrast agents for biological imaging: optical properties, surface conjugation and photothermal effects. *Photochemistry and photobiology*, *85*(1), 21-32.

(11) Lewinski, N., Colvin, V., & Drezek, R. (2008). Cytotoxicity of nanoparticles. *small*, *4*(1), 26-49.

(12) Chithrani, D. B. (2010). Intracellular uptake, transport, and processing of gold nanostructures. *Molecular membrane biology*, *27*(7), 299-311.

(13) Berry, C. C., & Curtis, A. S. (2003). Functionalisation of magnetic nanoparticles for applications in biomedicine. *Journal of physics D: Applied physics*, *36*(13), R198.

(14) Zhang, L. W., William, W. Y., Colvin, V. L., & Monteiro-Riviere, N. A. (2008). Biological interactions of quantum dot nanoparticles in skin and in

human epidermal keratinocytes. *Toxicology and applied pharmacology*, *228*(2), 200-211.

(15) Rothen-Rutishauser, B. M., Schürch, S., Haenni, B., Kapp, N., & Gehr, P. (2006). Interaction of fine particles and nanoparticles with red blood cells visualized with advanced microscopic techniques. *Environmental science & technology*, *40*(14), 4353-4359.

(16) Spangler, E. J., Harvey, C. W., Revalee, J. D., Kumar, P. S., & Laradji, M. (2011). Computer simulation of cytoskeleton-induced blebbing in lipid membranes. *Physical Review E*, *84*(5), 051906.

(17) Krčmar, M., Saslow, W. M., & Zangwill, A. (2003). Static screening by conducting nanospheres. *Journal of applied physics*, *93*(6), 3490-3494.

(18) Olinger, A. D., Kumar, P. B., & Laradji, M. (2017). Binding, Curvature-Sensing, Curvature-Generation and Self-Assembly of Anisotropically Curved Nanoparticles on Lipid Membranes. *Bulletin of the American Physical Society*, *62*.

(19) Zhang, S., Li, J., Lykotrafitis, G., Bao, G., & Suresh, S. (2009). Size-dependent endocytosis of nanoparticles. *Advanced materials*, *21*(4), 419-424.

(20) Zhang, S., Gao, H., & Bao, G. (2015). Physical principles of nanoparticle cellular endocytosis.

(21) Yuan, H., Huang, C., & Zhang, S. (2010). Virus-inspired design principles of nanoparticle-based bioagents. *PloS one*, *5*(10), e13495.

(22) Osaki, F., Kanamori, T., Sando, S., Sera, T., & Aoyama, Y. (2004). A quantum dot conjugated sugar ball and its cellular uptake. On the size effects of endocytosis in the subviral region. *Journal of the American Chemical Society*, *126*(21), 6520-6521.

(23) Chithrani, B. D., Ghazani, A. A., & Chan, W. C. (2006). Determining the size and shape dependence of gold nanoparticle uptake into mammalian cells. *Nano lett*, *6*(4), 662-668.

(24) Lewin, M., Carlesso, N., Tung, C. H., Tang, X. W., Cory, D., Scadden, D. T., & Weissleder, R. (2000). Tat peptide-derivatized magnetic nanoparticles allow in vivo tracking and recovery of progenitor cells. *Nature biotechnology*, *18*(4), 410-414.

(25) Tromsdorf, U. I., Bigall, N. C., Kaul, M. G., Bruns, O. T., Nikolic, M. S., Mollwitz, B., ... & Förster, S. (2007). Size and surface effects on the MRI relaxivity of manganese ferrite nanoparticle contrast agents. *Nano letters*, *7*(8), 2422-2427.

(26) Ding, H. M., & Ma, Y. Q. (2012). Role of physicochemical properties of coating ligands in receptor-mediated endocytosis of nanoparticles. *Biomaterials*, *33*(23), 5798-5802.

(27) Sperotto, M. M., & Ferrarini, A. (2017). Spontaneous Lipid Flip-Flop in Membranes: A Still Unsettled Picture from Experiments and Simulations. In *The Biophysics of Cell Membranes* (pp. 29-60). Springer, Singapore.

(28) Mouritsen, O. G. (2005). Life - as a matter of fat: The emerging science of lipidomics. Berlin: Springer.

(29) Alberts, B., Wilson, J. H., & Hunt, T. (1989). Molecular biology of the cell (5th ed.). New York: Garland Publishing.

(30) Bloom, M., Evans, E., & Mouritsen, O. (1991). Physical properties of the fluid lipid-bilayer component of cell membranes: A perspective. Quarterly Reviews of Biophysics, 24(3), 293-397. doi:10.1017/S0033583500003735

(31) Poursoroush, A., Sperotto, M. M., & Laradji, M. (2017). Phase behavior of supported lipid bilayers: A systematic study by coarse-grained molecular dynamics simulations. *The Journal of chemical physics*, *146*(15), 154902.

(32) RUANO, M. L., MIGUEL, E., PEREZ-GIL, J., & CASALS, C. (1996). Comparison of lipid aggregation and self-aggregation activities of pulmonary surfactant-associated protein A. *Biochemical Journal, 313*(2), 683-689.

(33) Pérez-Gil, J. (2008). Structure of pulmonary surfactant membranes and films: the role of proteins and lipid–protein interactions. *Biochimica et Biophysica acta (BBA)-Biomembranes*, *1778*(7), 1676-1695.

(34) Blanco, O., & Pérez-Gil, J. (2007). Biochemical and pharmacological differences between preparations of exogenous natural surfactant used to treat respiratory distress syndrome: role of the different components in an efficient pulmonary surfactant. *European journal of pharmacology*, *568*(1-3), 1-15.

(35) Parra, E., & Pérez-Gil, J. (2015). Composition, structure and mechanical properties define performance of pulmonary surfactant membranes and films. *Chemistry and physics of lipids*, *185*, 153-175.

(36) Garcia-Verdugo, I., Wang, G., Floros, J., & Casals, C. (2002). Structural analysis and lipid-binding properties of recombinant human surfactant protein a derived from one or both genes. *Biochemistry*, *41*(47), 14041-14053.

(37) Israelachvili, J. N., Mitchell, D. J., & Ninham, B. W. (1977). Theory of self-assembly of lipid bilayers and vesicles. *Biochimica et Biophysica Acta (BBA)-Biomembranes*, *470*(2), 185-201.

(38) Szoka Jr, F., & Papahadjopoulos, D. (1980). Comparative properties and methods of preparation of lipid vesicles (liposomes). *Annual review of biophysics and bioengineering*, *9*(1), 467-508.

(39) Cevc, G., & Blume, G. (1992). Lipid vesicles penetrate into intact skin owing to the transdermal osmotic gradients and hydration force. *Biochimica et Biophysica Acta (BBA)-Biomembranes*, *1104*(1), 226-232.

(40) Elsayed, M. M., Abdallah, O. Y., Naggar, V. F., & Khalafallah, N. M. (2007). Lipid vesicles for skin delivery of drugs: reviewing three decades of research. *International journal of pharmaceutics*, *332*(1-2), 1-16.

(41) Poste, G., & Papahadjopoulos, D. (1976). Lipid vesicles as carriers for introducing materials into cultured cells: influence of vesicle lipid

composition on mechanism (s) of vesicle incorporation into cells. *Proceedings of the National Academy of Sciences*, *73*(5), 1603-1607.

(42) Richard, C., Balavoine, F., Schultz, P., Ebbesen, T. W., & Mioskowski, C. (2003). Supramolecular self-assembly of lipid derivatives on carbon nanotubes. *Science*, *300*(5620), 775-778.

(43) Olinger, A. D., Spangler, E. J., Kumar, P. S., & Laradji, M. (2016). Membrane-mediated aggregation of anisotropically curved nanoparticles. *Faraday discussions*, *186*, 265-275.

(44) Simunovic, M., Šarić, A., Henderson, J. M., Lee, K. Y. C., & Voth, G. A. (2017). Long-Range Organization of Membrane-Curving Proteins. *ACS central science*, *3*(12), 1246-1253.

(45) McMahon, H. T., & Gallop, J. L. (2005). Membrane curvature and mechanisms of dynamic cell membrane remodelling. *Nature*, *438*(7068), 590.

(46) Chernomordik, L. V., & Kozlov, M. M. (2008). Mechanics of membrane fusion. *Nature Structural and Molecular Biology*, *15*(7), 675.

(47) Reynwar, B. J., Illya, G., Harmandaris, V. A., Müller, M. M., Kremer, K., & Deserno, M. (2007). Aggregation and vesiculation of membrane proteins by curvature-mediated interactions. *Nature*, *447*(7143), 461.

(48) Miller, S., & Krijnse-Locker, J. (2008). Modification of intracellular membrane structures for virus replication. *Nature Reviews Microbiology*, *6*(5), 363.

(49) Martin, I., Schaal, H., Scheid, A., & Ruysschaert, J. M. (1996). Lipid membrane fusion induced by the human immunodeficiency virus type 1 gp41 N-terminal extremity is determined by its orientation in the lipid bilayer. *Journal of virology*, *70*(1), 298-304.

(50) Sharma, M., Yi, M., Dong, H., Qin, H., Peterson, E., Busath, D. D., ... & Cross, T. A. (2010). Insight into the mechanism of the influenza A proton channel from a structure in a lipid bilayer. *Science*, *330*(6003), 509-512.

(51) Martín-Acebes, M. A., Merino-Ramos, T., Blázquez, A. B., Casas, J., Escribano-Romero, E., Sobrino, F., & Saiz, J. C. (2014). The composition of West Nile virus lipid envelope unveils a role of sphingolipid metabolism in flavivirus biogenesis. *Journal of virology*, *88*(20), 12041-12054.

(52) NOLL, H., & Youngner, J. S. (1959). Virus-lipid interactions. II. The mechanism of adsorption of lipophilic viruses to water-insoluble polar lipids. *Virology*, *8*(3), 319-43.

(53) Hu, J., Fu, R., Nishimura, K., Zhang, L., Zhou, H. X., Busath, D. D., ... & Cross, T. A. (2006). Histidines, heart of the hydrogen ion channel from influenza A virus: toward an understanding of conductance and proton selectivity. *Proceedings of the National Academy of Sciences*, *103*(18), 6865-6870.

(54) Rouser, G., Fleischer, S., & Yamamoto, A. (1970). Two dimensional thin layer chromatographic separation of polar lipids and determination of phospholipids by phosphorus analysis of spots. *Lipids*, *5*(5), 494-496.

(55) Laradji, M., & Kumar, P. S. (2004). Dynamics of domain growth in self-assembled fluid vesicles. *Physical review letters*, *93*(19), 198105.

(56) Lipowsky, R. (1992). Budding of membranes induced by intramembrane domains. *Journal de Physique II*, *2*(10), 1825-1840.

(57) Jülicher, F., & Lipowsky, R. (1996). Shape transformations of vesicles with intramembrane domains. *Physical Review E*, *53*(3), 2670.

(58) CASALS, C., RUANO, M. L., MIGUEL, E., SANCHEZ, P., & PEREZ-GIL, J. (1994). Surfactant protein-C enhances lipid aggregation activity of surfactant protein-A.

(59) Lewis, B. A., & Engelman, D. M. (1983). Lipid bilayer thickness varies linearly with acyl chain length in fluid phosphatidylcholine vesicles. *Journal of molecular biology*, *166*(2), 211-217.

(60) Needham, D., & Nunn, R. S. (1990). Elastic deformation and failure of lipid bilayer membranes containing cholesterol. *Biophysical journal*, *58*(4), 997-1009.

(61) Kagan, B. L., Selsted, M. E., Ganz, T., & Lehrer, R. I. (1990). Antimicrobial defensin peptides form voltage-dependent ion-permeable channels in planar lipid bilayer membranes. *Proceedings of the National Academy of Sciences*, *87*(1), 210-214.

(62) Korlach, J., Schwille, P., Webb, W. W., & Feigenson, G. W. (1999). Characterization of lipid bilayer phases by confocal microscopy and fluorescence correlation spectroscopy. *Proceedings of the National Academy of Sciences*, *96*(15), 8461-8466.

(63) Bretscher, M. S. (1972). Asymmetrical lipid bilayer structure for biological membranes. *Nature New Biology*, *236*(61), 11.

(64) Chiantia, S., & London, E. (2013). Lipid bilayer asymmetry. In *Encyclopedia of Biophysics* (pp. 1250-1253). Springer Berlin Heidelberg.

(65) Berndl, K., Käs, J., Lipowsky, R., Sackmann, E., & Seifert, U. (1990). Shape transformations of giant vesicles: extreme sensitivity to bilayer asymmetry. *EPL (Europhysics Letters)*, *13*(7), 659.

(66) Li, J., Yang, Y., & Huang, L. (2012). Calcium phosphate nanoparticles with an asymmetric lipid bilayer coating for siRNA delivery to the tumor. *Journal of controlled release*, *158*(1), 108-114.

(67) Schoch, P., Sargent, D. F., & Schwyzer, R. (1979). Capacitance and conductance as tools for the measurement of asymmetric surface potentials and energy barriers of lipid bilayer membranes. *The Journal of membrane biology*, *46*(1), 71-89.